Taylor & Francis
Taylor & Francis Group

Check for updates

Structural and simulation analysis of hotspot residues interactions of SARS-CoV 2 with human ACE2 receptor

Ganesh Kumar Veeramachaneni[a], V. B. S. C. Thunuguntla[b], Janakiram Bobbillapati[c] and Jayakumar Singh Bondili[a]

[a]Department of Biotechnology, Koneru Lakshmaiah Education Foundation (KLEF), Guntur, India; [b]Institute of Health and Sport, Victoria University, Melbourne, Australia; [c]Department of Microbiology, NRI Medical College and General Hospital, Guntur, India

Communicated by Ramaswamy H. Sarma

ABSTRACT

The novel corona virus disease 2019 (SARS-CoV 2) pandemic outbreak was alarming. The binding of SARS-CoV (CoV) spike protein (S-Protein) Receptor Binding Domain (RBD) to Angiotensin converting enzyme 2 (ACE2) receptor initiates the entry of corona virus into the host cells leading to the infection. However, considering the mutations reported in the SARS-CoV 2 (nCoV), the structural changes and the binding interactions of the S-protein RBD of nCoV were not clear. The present study was designed to elucidate the structural changes, hot spot binding residues and their interactions between the nCoV S-protein RBD and ACE2 receptor through computational approaches. Based on the sequence alignment, a total of 58 residues were found mutated in nCoV S-protein RBD. These mutations led to the structural changes in the nCoV S-protein RBD 3d structure with 4 helices, 10 sheets and intermittent loops. The nCoV RBD was found binding to ACE2 receptor with 11 hydrogen bonds and 1 salt bridge. The major hot spot amino acids involved in the binding identified by interaction analysis after simulations includes Glu 35, Tyr 83, Asp 38, Lys 31, Glu 37, His 34 amino acid residues of ACE2 receptor and Gln 493, Gln 498, Asn 487, Tyr 505 and Lys 417 residues in nCoV S-protein RBD. Based on the hydrogen bonding, RMSD and RMSF, total and potential energies, the nCoV was found binding to ACE2 receptor with higher stability and rigidity. Concluding, the hotspots information will be useful in designing blockers for the nCoV spike protein RBD.
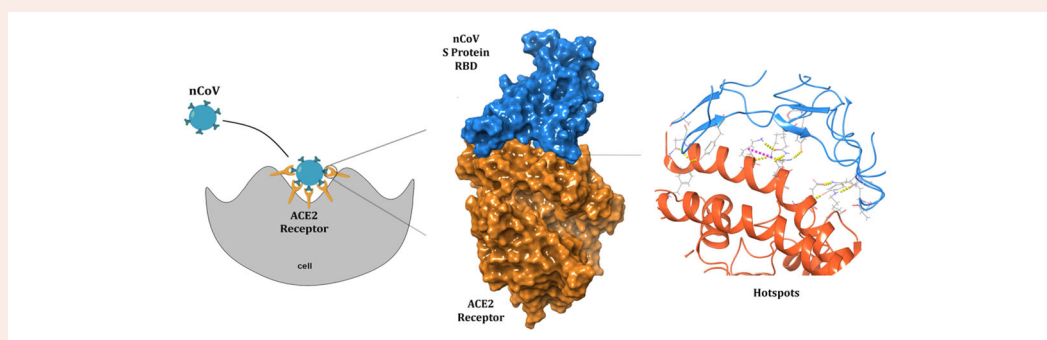
1. Introduction

The emergence of highly pathogenic novel coronavirus in 2019 (SARS-CoV 2) became pandemic and posed a global health emergency. The Coronaviridae family viruses are mostly hosted by animals and are found pathogenic to humans. Though these viruses were pathogenic to humans, most of them caused mild to moderate symptoms (Lu et al., 2020). However, Severe Acute Respiratory Syndrome (SARS) in 2002 and the MERS (Middle East Respiratory Syndrome) in 2012 caused by SARS-CoV (CoV), infected larger populations and showed significant fatalities. In December 2019, another

beta-Coronavirus has been identified in a group of people admitted with severe pneumonia symptoms in Wuhan, China named as SARS-CoV 2 (nCoV) (Lu et al., 2020; Muralidharan et al., 2020; Peeri et al., 2020; Umesh et al., 2020; Wahedi et al., 2020; Zhou & Zhao, 2020). In a short span of time, the infection rate increased with ∼4.2 million people infected and 0.29 million deaths by 14th May 2020 throughout the world (WHO, 2020) and continuing. Many of the countries adopted social distancing and lock down precautions to decrease the rate of nCoVID-19 infections from human to human but for the lack of vaccines and targeted therapies (Aanouz et al., 2020; Elfiky, 2020a; Kumar et al., 2020).
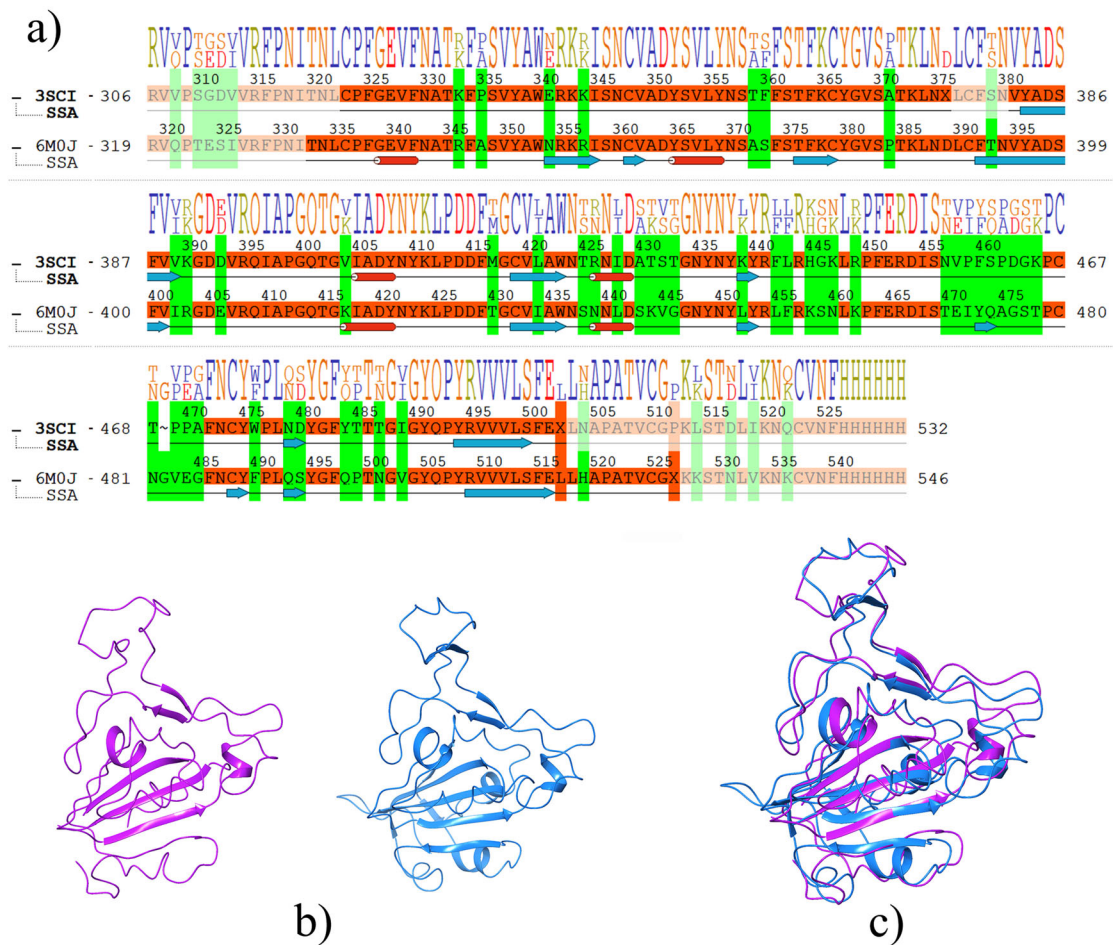
CONTACT Jayakumar Singh Bondili ✉ jksingh@kluniversity.in 📧 Department of Biotechnology, Koneru Lakshmaiah Education Foundation (KLEF), Green Fields, Vaddeswaram, Guntur, India

Figure 1. Multiple sequence alignment (MSA) of Spike protein of SARS-CoV (P59594) and nCov (P0DTC2). The Receptor Binding Domain (RBD) region is highlighted in the box.

The phylogenetic analysis states that SARS-CoV 2 (nCoV) is closely related to bat derived coronavirus bat-SL-CoVZC45 and bat-SL-CoVZXC21 (Han et al., 2006; Lan et al., 2020; Lu et al., 2020). It is known that, different coronaviruses can start an infection by binding spike glycoprotein subunit to specific receptors of the human cells. For instance, MERS-CoV binds to CD26 and N-terminal end of SARS-CoV spike protein Receptor Binding Domain (RBD) binds to Angiotensin converting enzyme 2 (ACE2) receptors (Abdelli et al., 2020; Al-Khafaji et al., 2020; Hasan et al., 2020; Khan, Jha, et al., 2020; Lan et al., 2020; Peeri et al., 2020; Yan et al., 2020). The ACE2 interaction promotes spike protein subunit S2 for membrane perfusion by dissociation of the Receptor Binding Domain (RBD) of subunit S1 after interaction with ACE2 (Boopathi et al., 2020; Hasan et al., 2020). The CoV structure includes, Matrix protein (M-protein), small Envelop protein (E-protein) (Gupta et al., 2020), Spike (S) glycoprotein, Nucleocapsid protein (N-Protein) (Elfiky, 2020b) and other proteins like chymotrypsin (Elmezayen et al., 2020),

papain like proteases (Joshi et al., 2020; Khan, Zia, et al., 2020; Sarma et al., 2020). The Spike protein initiates binding with host cell receptor system and N-protein plays a crucial role of RNA replication in the host cells (Enayatkhani et al., 2020; Lobo-Galo et al., 2020; Sarma et al., 2020). The structural similarity between SARS-CoV and nCoV strengthens the binding of nCoV spike protein with ACE2 receptor possibilities (Adeoye et al., 2020; Lan et al., 2020). However, the antibodies raised against SARS-CoV recovered people were not able to neutralize nCoVID-19 symptoms (Lan et al., 2020). This signifies the structural differences of the nCoV from CoV.

The recently published crystal structure (PDB Id: 6M0J) elucidates the structural interactions of spike protein RBD of nCoV. Considering that there are extended mutations present in the nCoV sequence, which comes under RBD (Sinha et al., 2020), it has been shown that more ACE2 interacting residues were present in the nCoV spike protein RBD than CoV (Lan et al., 2020; Pant et al., 2020). It is important to understand the hot spot

Figure 2. Multiple sequence alignment and superimposition of CoV spike protein RBD (PDB Id: 3SCI: chain E) and nCoV spike protein RBD (PDB Id: 6M0J: chain E). a) MSA of CoV spike protein RBD and nCoV spike protein RBD (blue colored arrows signify sheets, orange color cylinder shapes are helices and black line represents loops). b) 3d structures of CoV spike protein RBD (purple) and nCoV spike protein RBD (blue) and c) Super imposition CoV spike protein RBD (purple) and nCoV spike protein RBD (blue).

Table 1. List of helices and sheets in the CoV and nCoV S-protein RBD.

SARS−CoV		SARS−nCoV	
Helix	Sheets	Helix	Sheets
Ile 405 – Tyr 408	Tyr 383 – Val 389	Gly 339 – Phe 342	Asn 354 – Ile 358
Arg 426 – Asp 429	Cys 419 – Trp 423	Tyr 365 – Tyr 369	Cys 361 – Val 362
	Lys 439 – Tyr 440	Lys 417 – Tyr 421	Thr 376 – Cys 379
	Asn 479 – Asp 480	Asn 439 – Asp 442	Phe 392 – Val 401
	Tyr 494 – Ser 500		Cys 432 – Trp 436
			Leu 452 – Tyr 453
			Tyr 473 – Gln 474
			Cys 488 – Tyr 489
			Gln 493 – Ser 494
			Arg 509 – Glu 516

amino acids and their interactions and how far these interactions are stable allowing the membrane perfusion of virus into the host cell. The current *in silico* study focuses on, highlighting the ACE2 and spike protein RBD amino acid interactions. The strength of the hot spot amino acid interactions were studied through molecular dynamic simulations for a period of 100 ns. The deviations and fluctuations made by the ACE2-RBD complex along with energies clarify in understanding the stability of the nCoV spike protein RBD interaction with ACE2 receptor in comparison to SARS-CoV.

2. Materials and methods

The entire computational work was performed using the Schrodinger suite. The applications employed in the present study are

2.1. Multiple sequence alignment

The mapping of S protein RBD sequences of both CoV and nCoV was performed using the multiple sequence viewer tool of the prime application of Schrodinger suite.
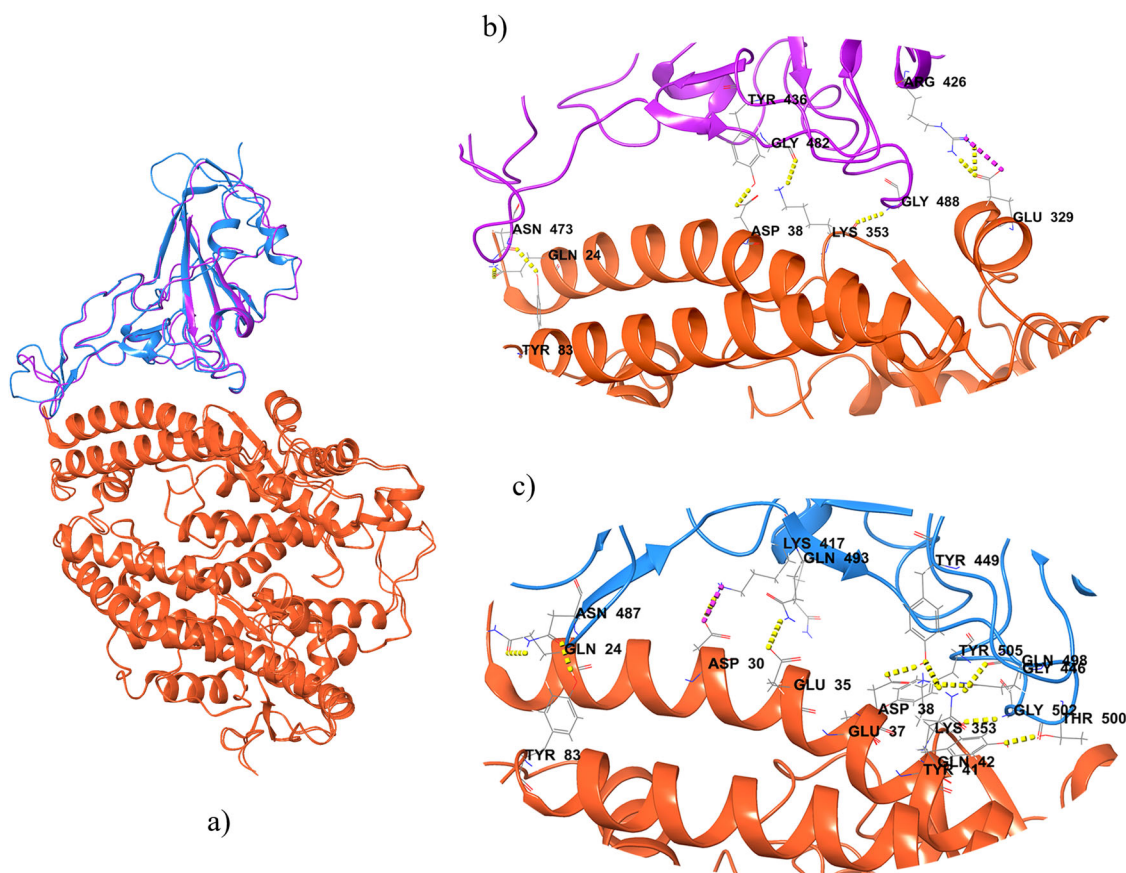
Figure 3. Superimposition of ACE2-CoV S-protein RBD complex (PDB Id: 3SCI) with ACE2-nCoV S-protein RBD complex (PDB Id: 6M0J) and interaction profiles. a) Superimposition of ACE2 (orange) - CoV S-protein RBD (purple) with ACE2 (orange) - nCoV S-protein RBD (purple). b) Interactions between ACE2 receptor and CoV S-protein RBD. c) Binding profiles of ACE2 receptor and nCoV S-protein RBD.

2.2. Protein preparation wizard

The crystal structures were retrieved from protein databank and prepared using protein preparation wizard tool. The parameters used in refining the structure are addition of hydrogen's, creating disulphide bonds, maintaining zero order bonds and selenomethionines to methionines conversion in the import and process tab. Further, in refine tab, optimizing the hydrogen bonds to repair and finally minimized the structure through force field OPLS_2005. Using superimposition tool of the maestro, both complexes (CoV and nCoV-ACE2) and individual S-protein RBD of both CoV and nCoV were structurally superimposed and their RMSD (Root Mean Square Deviations) was calculated (Jorgensen et al., 1996; Sastry et al., 2013; Veeramachaneni et al., 2015; Veeramachaneni et al., 2015).

2.3. Molecular dynamics simulations

Molecular dynamic simulations (MDS) of the complexes were performed using Desmond software. Initially, the complex was imported into the system builder application of Desmond module and with default parameters like SPC (simple point-charge) solvent model, orthorhombic periodic boundary box (Box size; distances (Å): a:10 × b:10 × c:10 and Angles: α:900 × β:900 × γ:900) and minimizing the volume, a model system was generated for simulations. Continuing with the ions tab of system builder application, Na$^+$ ions were added based on the total charge and a salt concentration of 0.15 M was also added

to neutralize the system. Second step in the simulations protocol was minimization, the complex obtained from the system builder was relaxed by setting the maximum iterations number to 2000 and remaining parameters were set to default. Finally, the minimized complex was subjected to molecular dynamic simulations by setting the ensemble parameter to NPT [isothermal–isobaric ensemble, Number of particles (N), Pressure (P) and Temperature (T)], 300 K temperature, 1 bar pressure, simulation run time was set to 100 ns (Islam et al., 2020) and relaxed using the default relation protocol (Guo et al., 2010; Veeramachaneni et al., 2019).

2.4. Protein binding analysis

Protein binding analysis was performed using the protein interaction analysis application of the Schrodinger suite.

3. Results and discussion

3.1. Sequence analysis of SARS-Corona virus and SARS-Corona virus-2 spike protein

Spike protein (S-protein) sequence of SARS-CoV (CoV) and SARS-CoV 2 (nCoV) were retrieved from the uniprot databank with sequence IDs P59594 and P0DTC2 respectively. The multiple sequence alignment was performed using Clustal omega web server of EMBL-EBI services. The

Table 2. Interaction profiles of spike protein RBD.

a) Data representing the interaction profile of CoV (PDB Id: 3SCI) after proteins interaction analysis

CoV S protein RBD	ACE2 receptor	Distance	Specific Interactions	Buried SASA
Arg 426	Glu 329	2.9 A	2 HB, 1SB to Glu 329	51.20%
	Gln 325	3.6 A		
Tyr 436	Asp 38	2.7 A	1HB to Asp 38	38.20%
	Gln 42	3.3 A		
Asn 473	Gln 24	3.0 A	1HB to Gln 24	65.30%
	Tyr 83	3.1 A	1HB to Tyr 83	
Gly 482	Lys 353	3.0 A	1HB to Lys 353	91.80%
Tyr 484	Gln 42	3.1 A	1pi stack to Tyr 41	97.30%
	Leu 45	3.5 A		
	Tyr 41	3.6 A		
	Asp 38	4.0 A		
Gly 488	Lys 353	3.0 A	1HB to Lys 353	93.50%
	Gly 354	3.4 A		

b) The interaction profiles of nCoV (PDB Id: 6M0J) amino acids after proteins interaction analysis.

nCoV S protein RBD	ACE2 receptor	Distance	Specific Interactions	Buried SASA
Lys 417	Asp30	2.7 A	1HB, 1SB to Asp 30	37.10%
Gly 446	Gln 42	3.1 A	1HB to Gln 42	20.10%
Tyr 449	Asp 38	2.8 A	1HB to Asp 38	29.40%
	Gln 42	3.0 A	1HB to Gln 42	
Asn 487	Tyr 83	2.8 A	1HB to Gln 24	91.20%
	Gln 24	3.0 A	1HB to Tyr 83	
Gln 493	Glu 35	3.1 A	1HB to Glu 35	78.30%
	Lys 31	3.5 A		
Gln 498	Lys 353	3.3 A	1HB to Lys 353	99.80%
	Gln 42	3.4 A		
	Tyr 41	3.5 A		
	Asp 38	3.8 A		
Thr 500	Tyr 41	2.8 A	1HB to Tyr 41	76.20%
	Asp 355	3.2 A		
	Asn 330	3.3 A		
	Arg 357	3.5 A		
Gly 502	Lys 353	3.0 A	1HB to Lys 353	93.30%
	Gly 354	3.5 A		
Tyr 505	Glu 37	2.9 A	1HB to Glu 37	78.50%
	Lys 353	3.5 A		
	Arg 393	3.5 A		
	Gly 354	3.8 A		

alignment results displayed 75.9% identity (Figure 1) between the sequences. Previous studies (Aydin et al., 2014) reported the Receptor Binding Domain (RBD) of the CoV spike protein ranging from 306 to 527 and in specific the residues 424–494 related to binding motif played a crucial role in binding to the human ACE2 receptor for viral admittance. In nCoV, these residues were aligned at 319–541 and 437–508 positions respectively. The spike protein RBD of CoV and nCoV shared only 74% identity. The alignment displayed 26% mutations and 58 residues were found mutated in the spike protein RBD region of nCoV. Among these, 34 mutations related to the binding motif were predicted as the crucial amino acids based on the correlation analysis done with the spike protein binding motif of CoV. Considering this binding region as a major criterion, the CoV and nCoV receptor binding domains were further analyzed for any structural changes resulting out of these mutations.

3.2. Structural analysis of CoV and nCoV receptor binding domain

To continue the structural analysis of the receptor binding regions, reported PDB structures of SARS-CoV (PDB Id: 3SCI) and SARS-nCoV (PDB Id: 6M0J) were retrieved from the protein databank. The F-chain in both the sequences relates to the spike protein RBD of the virus and the A-chain represents ACE2 receptor. Prior to the analysis, RBD sequences retrieved (PDB) were cross validated against their corresponding full length uniprot sequences. Many structural modifications were observed in the nCoV RBD of Spike protein because of the mutations occurred during the course of time compared to the CoV. The overview of the mutational changes in the secondary structure of both CoV and nCoV spike protein receptor binding region were aligned in Figure 2(a). In CoV, the majority of the spike protein RBD 3d structure was made of loops with 2 helices and 5 sheets. While, the 3d structure of nCoV spike protein RBD comprised of 4 helices and 10 sheets with interconnecting loops (Figure 2(b)) (Lan et al., 2020).

The detailed information regarding the residues involved in the helices and sheets of both the proteins were tabulated (Table 1). The major structural changes recorded were seen in the residues ranging from 306 to 382 of CoV which were in the loop region while the corresponding residues of nCoV i.e. 333–395 were framed into two helices and three sheets. The helix observed in the CoV protein (426–429) was absent in the corresponding nCoV (439–442 residues) and these residues were sited in loop region. Extra sheets in nCoV protein between Tyr 473-Gln 474, Cys 488-Tyr 489 and Val 524-Cys
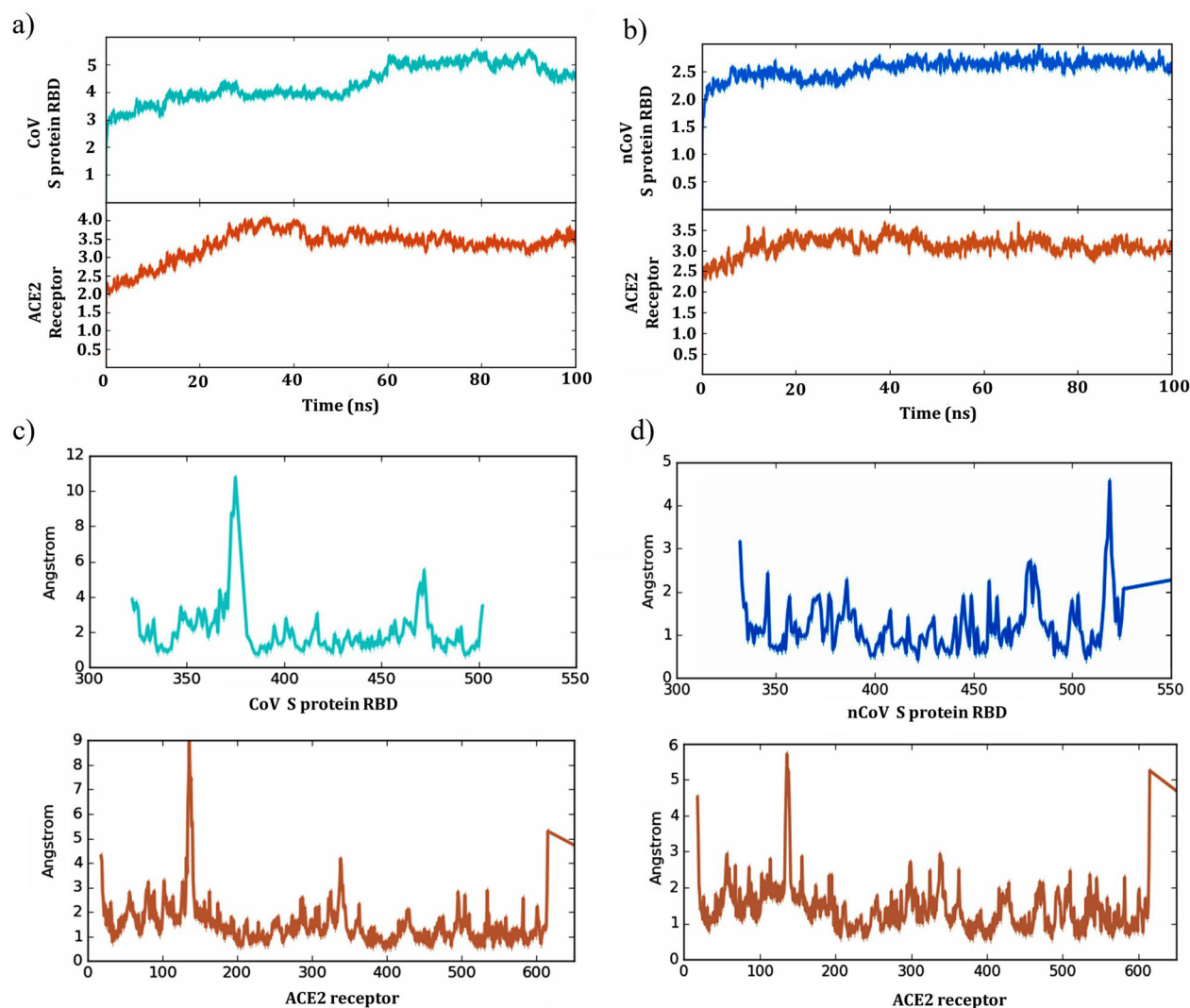
Figure 4. Molecular dynamic simulation analysis of ACE2-CoV S-protein RBD and ACE2- nCoV S-protein RBD a) Deviations graph of ACE2 receptor and CoV S-protein RBD. b) RMSD graphs of ACE2 receptor and nCoV S-protein RBD. c) RMSF graph of ACE2 receptor and CoV S-protein RBD. d) ACE2 receptor and nCoV S-protein RBD residues fluctuation graph.

525 were absent in CoV and these residues were shaped into loops.

3.3. Binding modes of CoV and nCoV spike protein receptor binding domain with ACE2 receptor

The complex of the ACE2 receptor with RBD of the CoV and nCoV spike protein crystal structures were retrieved and prepared using the protein preparation wizard application of the Schrodinger suite through a series of steps as explained in the methodology part. The prepared complexes were subjected to protein interaction analysis application available in the suite to investigate the interactions occurring between the receptor and spike protein RBD. The superimposition of CoV and nCoV without ACE2 receptor resulted in 7.37 Å RMSD (Figure 2(c)) and in complex with ACE2 receptor, the superimposed complexes were displaying 15.24 Å deviations (RMSD) (Figure 3(a)).

The CoV RBD-ACE2 complex was maintained with 7 Hydrogen bonds, 1 pi-pi interaction and 1 Salt bridge (Figure

3(b)). Concurrently, the nCoV spike protein RBD-ACE2 receptor complex displayed 11 hydrogen bonds and 1 salt bridge (Figure 3(c)). Interactions like hydrogen bond, pi-pi stacking and salt bridge made by the CoV and nCoV spike protein with ACE2 receptor were reported along with their closest residues, distance and also the solvent accessible surface area (SASA) (Table 2). In both the complexes, residues 473/487, 436/449 and 473/487 of virus RBD maintained hydrogen bond interaction profiles with the residues 24, 38 and 83 of the ACE2 receptor respectively. Prime/MM–GBSA based binding-free energy was calculated by considering nCoV and CoV as ligands against the ACE2 receptor. The binding-free energies calculated were −126.5 kcal/mol for nCoV and −100.2 kcal/mol with CoV. Comparing the two complexes binding interaction profiles, nCoV was found binding more rigidly to the ACE2 receptor than CoV with more number of H bonds and the binding free energy calculations were also found inline supporting the interaction analysis results confirming nCoV binding with more stringency to the human ACE2 receptor when compared to CoV.
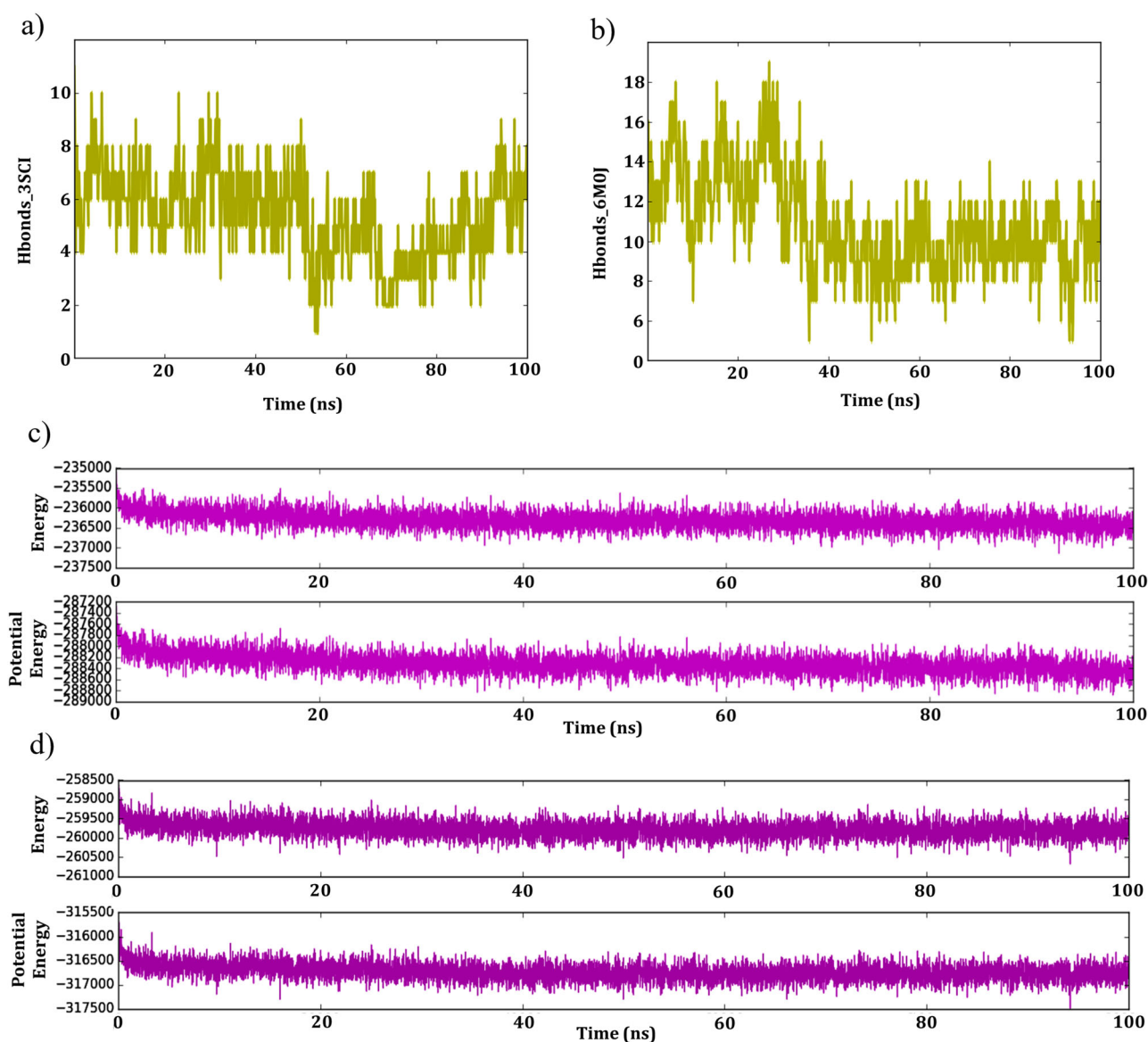
Figure 5. Hydrogen bond and energies reported by the ACE2-CoV S-protein RBD (3SCI) and ACE2-nCoV S-protein RBD (6M0J) after simulations. a) Hydrogen bonds graph maintained by the receptor and protein during simulation run b) ACE2 receptor and S-protein RBD of nCoV complex hydrogen bonds graph after simulations studies. c) Average energy and potential energies graph of ACE2-CoV S-protein RBD complex and d) Average energy and potential energies graph of ACE2-nCoV S-protein RBD complex.

3.4. Molecular dynamic simulations

Both the crystal structures were subjected to molecular dynamic simulation studies over a period of 100 ns to understand the stability of the complexes. Hydrogen bond interactions, Root-Mean-Square Deviation (RMSD) and Root-Mean-Square Fluctuation (RMSF) made by CoV and nCoV with the ACE2 receptor in complex state and their binding profiles were analyzed. The average total energy and potential energy of the complexes were also calculated to evaluate the rigidity of the complexes.

3.4.1. Deviations analysis

Using the trajectories of the complex, the deviations made by the two spike proteins were reported individually. The deviations made by the ACE2 receptor and spike protein RBD of CoV complex (3SCI) were displayed in the Figure 4(a). In the initial simulation period until 30 ns, the ACE2 receptor

deviations were found in the inclined state and thereafter the protein maintained stable deviations till the end of the simulation run time (100 ns). The deviation range was between 2.0 and 4.0 Å while majority of the deviations were around 3.5 Å. The spike protein RBD inclined deviations were observed throughout the simulation run time and the deviations were in the range of 3.0–5.0 Å.

In the ACE2 - nCoV spike protein RBD complex (6M0J), the ACE2 receptor made deviations between 2.5 and 3.5 Å and majority of the deviations were maintained around 3.0 Å. From 20 ns of simulation run time, steady state in the deviations with small fluxes were observed till the end of 100 ns (Figure 4(b)). Based on the acceptable deviation range i.e. 2–3 Å, the deviations made by the ACE2 receptor reflects the stability of the receptor in the complex form. The deviations made by the nCoV spike protein RBD were low raging between 2.0 and 3.0 Å only. The stability in the deviations

Table 3. Number of hydrogen bonds maintained by ACE2 receptor - nCoV S-protein RBD complex during dynamic simulations intervals and its RMSD values.

Time Step (ns)	No. of Hbonds	RMSD (Å)	
		ACE2 receptor	nCoV S protein RBD
10.00	10.00	3.54	2.56
20.00	16.00	3.48	2.51
30.00	11.00	3.30	2.33
40.00	10.00	3.39	2.56
50.00	8.00	3.20	2.63
60.00	11.00	3.30	2.57
70.00	10.00	3.20	2.73
80.00	10.00	3.03	2.64
90.00	11.00	3.09	2.65
100.00	12.00	3.17	2.65

Table 4. Interactions profile between nCoV S-protein RBD with the residues of ACE2 receptor during the course of 100 ns simulation run time.

nCoV S-protein RBD	ACE2 receptor
408	387
417	30,34
446	42
449	38
453	34
475	19,24
484	31
487	83
489	24,27,83
490	31
492	31,83
493	31,34,35
496	353
498	38,353
500	41,42,355
501	41,353
502	353
505	37,353

Table 5. List of important residues identified in ACE2 receptor and their hydrogen bond interactions sustained during the 100 ns simulation run time.

MDS run time (ns)	ACE2 receptor residues
10, 20, 30, 40, 50, 60, 70, 80, 90, 100	Glu 35
10, 20, 30, 40, 60, 70, 80, 90, 100	Tyr 83
10, 20, 40, 50, 60, 70, 80, 90, 100	Asp 38
10, 20, 40, 60, 70, 80, 90, 100	Lys 31
20, 40, 50, 60, 70, 80, 90, 100	Glu 37
30, 40, 50, 60, 70, 80, 90, 100	His 34
10, 20, 30, 40, 70, 90, 100	Lys 353
30, 40, 50, 60, 70, 80, 100	Asp 30
10, 30, 50, 60, 80	Gln 24
30, 70, 80, 90, 100	Gln 42
10, 20, 30, 40	Thr 27
10, 20, 30	Tyr 41
20, 60	Ser 19
10	Asp 355
50	Ala 387

Table 6. Identified important residues in nCoV S-protein RBD and their hydrogen bond interactions sustained during the 100 ns simulation run time.

MDS run time (ns)	nCoV Spike protein RBD residues
10, 20, 30, 40, 50, 60, 70, 80, 90, 100	Gln 493
10, 20, 30, 40, 60, 70, 80, 90, 100	Gln 498
10, 20, 30, 40, 60, 80, 90, 100	Asn 487
20, 40, 50, 60, 70, 80, 90, 100	Tyr 505
30, 40, 50, 60, 70, 80, 90, 100	Lys 417
10, 20, 30, 70, 80, 90, 100	Thr 500
10, 20, 30, 40, 70, 100	Tyr 489
10, 20, 40, 70, 90, 100	Asn 501
40, 50, 60, 80, 90, 100	Tyr 453
20, 30, 50, 60, 80	Ala 475
20, 70, 90, 100	Leu 492
10, 20, 30	Gly 502
20, 40, 90	Phe 490
20, 30	Gly 496
60, 80	Glu 484
30	Gly 446
50	Arg 408, Tyr 449

was attained from the 40 ns run time and maintained the pace till the end of the simulation run. Comparing the two complexes based on the RMSD results, the ACE2-nCoV was found more stable compared to the ACE2-CoV complex. The spike protein RBD of CoV and nCoV deviations difference was 2.0–2.5 Å which is higher when compared to the ACE2 receptor with a change of around 0.5–1 Å only. The receptor made deviations were almost similar in both the complexes while the difference in the deviations made by CoV and nCoV spike protein RBD could be attributed to mutations and structural changes.

3.4.2. Residues fluctuation analysis

Fluctuations made by the ACE2 receptor and CoV spike protein RBD were depicted in the Figure 4(c). The range of the ACE2 receptor residues fluctuation with CoV was between 0.5 and 3.0 Å while the majority of the residues fluctuated between 1 and 2Å. Interestingly, the residues of the ACE2 receptor in complex with nCoV spike protein RBD also produced a similar type of fluctuation range i.e. 0.5–3.0 Å (Figure 4(d)). CoV spike protein RBD showed fluctuations ranging 0.5–4 Å with average fluctuations around 2.0 Å while nCoV spike protein RBD fluctuations were reported between 0.5 and 2.8 Å and the majority of the residues fluctuated around 1.5 Å. The tail end residue fluctuations were also observed as expected. In conclusion, considering all the fluctuations made by the spike protein RBD in both

the complexes, the nCoV residues fluctuations range was low, leading to more stability and rigidity of the complex.

3.4.3. Hydrogen bonds and energy

Using the trajectories and simulation event analysis, the number of hydrogen bonds formed between the complexes during the simulation runs was calculated. In ACE2-CoV spike protein RBD complex (PDB: 3SCI) the hydrogen bond range was 1–11 and mean value (average number of hydrogen bonds) was 5 (Figure 5(a)). Similarly in ACE2-nCoV spike protein RBD complex (PDB: 6M0J) the range was 5–19 and the mean value was 11 (Figure 5(b)). Using the simulation quality analysis tool, the total and potential energies of the two complexes were calculated. The CoV complex reported with −236309.88 and −288318.27 kcal/mol of total and potential energy whereas nCoV showed −259769.80 and −316730.74 kcal/mol respectively (Figure 5(c, d)). These values state that the nCoV complex was more stable compared to the CoV complex justifying the increase in the average number of hydrogen bond.

3.4.4. Identification of crucial residues involved in hydrogen bonding: ACE2-nCoV

The main aim of this interaction profile study was to elucidate the residues (hotspots) in both the receptor and S-
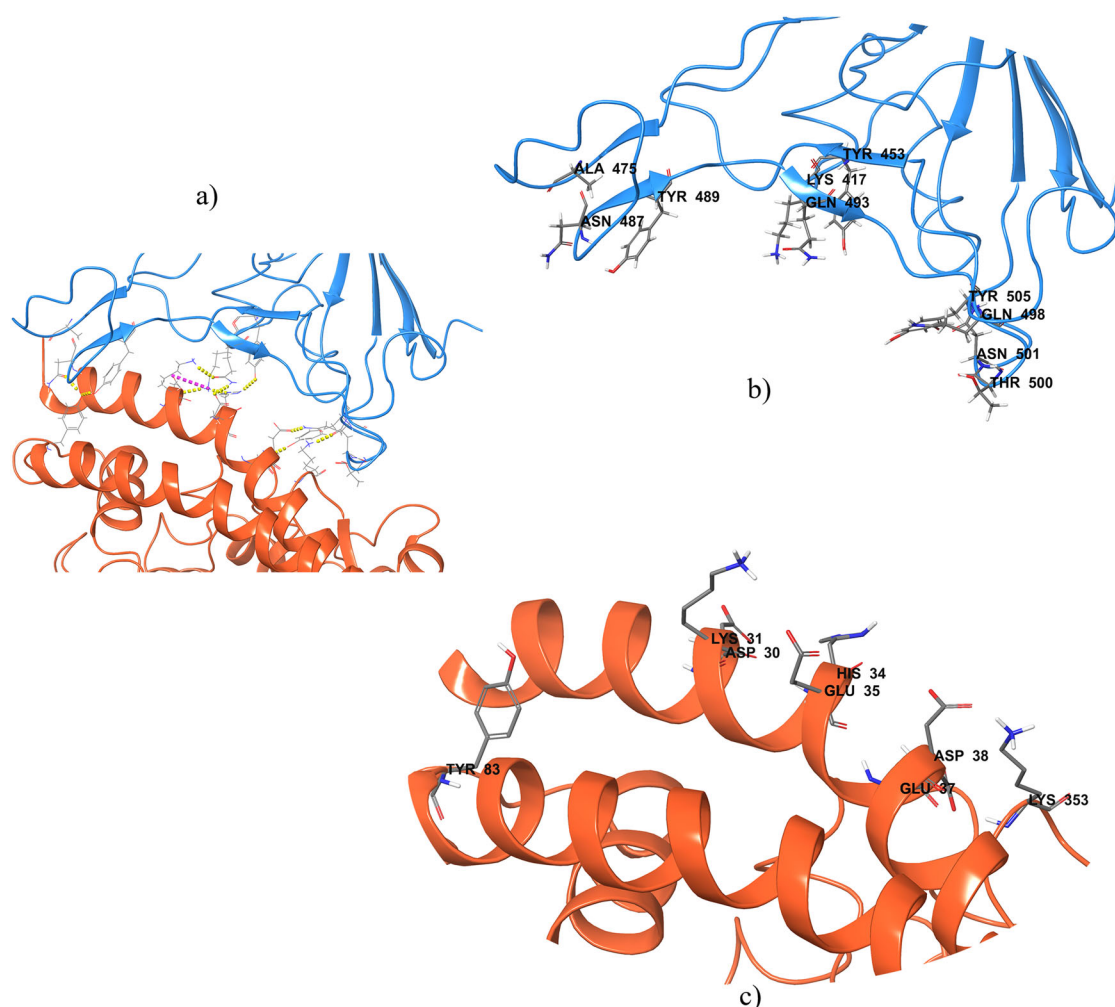
Figure 6. Interaction profiles of ACE2 and nCoV S-protein RBD after simulations and their hotspots a) Binding profile of ACE2-nCoV S-protein RBD complex after 100 ns simulation run. b) Hotspots of nCoV S-protein RBD. c) Important hotspot residues identified in ACE2 receptor.

protein and their interactions. Using the trajectory file, at every 10 ns of simulation run time interval, poses were considered for the binding analysis study. A total of 10 frames were retrieved and the residues which were involved in hydrogen bond formation in both ACE2 receptor and spike protein RBD of nCoV were identified (Table 3).

During the simulation run, some residues which were involved in the hydrogen bonding in the initial time intervals failed to continue the same bond in the succeeding intervals and were later found again retaining their interactions by the end of the simulation. Simultaneously, some of the residues which failed to produce hydrogen bond in the initial time frames were later found establishing and continuing with the established hydrogen bond by the end of the simulation run. Based on the results, 18 amino acids of nCoV Spike protein and 15 residues of the ACE2 receptor were identified showing stable hydrogen bond formation (Table 4).

The hydrogen bonds were characterized into strong (2.2–2.5 Å), moderate (2.5–3.2 Å) and weak (3.2–4.0 Å) based on the distance between the donor and acceptor (Jeffrey & Jeffrey, 1997; Khan, Jha, et al., 2020). Based on this, majority of the reported hydrogen bonds between ACE2 receptor residues with nCoV spike protein RBD were under moderate

category. The interaction percentage (100% correlating to the hydrogen bond sustainability in all the selected 10 frames) of the ACE2 receptor residues with nCoV spike protein RBD were Glu 35: 100% which preserved hydrogen bond interaction in all selected frames; Tyr 83 and Asp 38: 90%; three residues Lys 31, Glu 37 and His 34: 80%; followed by Lys 353 and Asp 30: 70%; Gln 24 and Gln 42: 50% and the remaining other five residues reported below 50% hydrogen bond sustainability (Table 5).

The corresponding nCoV amino acid residues involved in the hydrogen bonding with the receptor during the simulation studies were also identified (Table 6). Residue Gln 493 showed 100% hydrogen bonding throughout the simulation. Other residues hydrogen bond interaction percentage were Gln 498: 90%; Asn 487, Tyr 505 and Lys 417: 80%; followed by Tyr 489, Asn 501 and Tyr 453:60% and Ala 475:50%. Apart from these, the remaining other nine residues reported below 50% hydrogen bonding interaction percentage.

During simulations, some hydrogen bonds between nCoV S-protein RBD and ACE2 receptor residues were intact throughout the run time while certain residues showed shift in the hydrogen bonds. Interestingly, top listed residue Gln 493 of nCoV S-protein and Glu 35 of receptor were maintained hydrogen throughout the simulation. In addition, Gln

493 also maintained another hydrogen bond with Lys 31(70%) of the receptor and hence based on these observations Gln 493 was reported as the crucial residue in nCoV binding. Residue Gln 498 was seen maintaining an overall 90% hydrogen bond interaction shared with Asp 38 (70%) and in some intervals shifted to Lys 358 (20%).

Third residue in the nCoV S-protein RBD was Asn 487 which maintained its 90% of interaction profile with Tyr 83. Simultaneously, a shift in the H bond was also found among the residues like Lys 31 of receptor forming hydrogen bonds with Phe 490, Leu 492 and Glu 484 of the S-protein during the entire simulation period. These changes could be attributed to the flexibility nature of both receptor and S-protein during the course of the simulations run. CoV S-protein RBD residues 436, 473, 475, 479, 481, 482, 486, 487, 488 and 491 were previously reported as hotspots in several studies (Han et al., 2006; Wan et al., 2020). In the present study, comparing the hotspots of CoV and nCoV it can be stated that most of the hotspots of CoV were replicated in nCoV too. Among them, two residues Asn 479/Thr 487 of CoV were found mutated to Gln 493/Asn 501 in nCoV. These mutated amino acid residues were found having H bond interactions Gln493 (100%) and Asn 501(60%) during the simulations and profoundly influenced the binding to S-protein RBD to ACE2 receptor. The important hot spots identified in ACE2 receptor and nCoV S-protein RBD after simulation studies were displayed in the Figure 6. Along with the hydrogen interactions, hydrophobic interactions between the nCoV S-protein RBD and ACE2 receptor were also analyzed in the time frames defined (Tina et al., 2007). Based on the analysis, Leu 79, Met 82, Tyr 83, Phe 28of ACE2 receptor and Phe 486, Tyr 489 of nCoV S protein RBD were found involved in the hydrophobic interactions.

4. Conclusions

In conclusion, this study reports the hotspot amino acid residues involved in the binding of the nCoV spike protein RBD with human ACE2 receptor. Overall, the mutations identified in nCoV spike protein receptor binding domain had led to structural changes with additional sheets and helices in the RBD structure facilitating more H bond interactions between the ACE2 receptor and spike protein. The hotspot residues interactions were listed and the RMSD and RMSF of the 100 ns simulation run confirms the stability and rigidity of the interactions. The energy calculations reiterate the binding efficiency of the nCoV in comparison to CoV. Further, considering these hotspot amino acid residues, blockers could be designed for inhibiting the binding of nCoV spike protein RBD to human ACE2 receptor and thereby stopping the entry of the virus into the host cells.

Acknowledgements

Disclosure statement

Author contributions

References

Aanouz, I., Belhassan, A., El Khatabi, K., Lakhlifi, T., El Idrissi, M., & Bouachrine, M. (2020). Moroccan Medicinal plants as inhibitors of COVID-19: Computational investigations. *Journal of Biomolecular Structure and Dynamics (Just-Accepted)*, 1–12. https://doi.org/10.1080/07391102.2020.1758790

Abdelli, I., Hassani, F., Bekkel Brikci, S., & Ghalem, S. (2020). In silico study the inhibition of Angiotensin converting enzyme 2 receptor of COVID-19 by Ammoides verticillata components harvested from western Algeria. *Journal of Biomolecular Structure and Dynamics (Just-Accepted)*, 1–17. https://doi.org/10.1080/07391102.2020.1763199

Adeoye, A. O., Oso, B. J., Olaoye, I. F., Tijjani, H., & Adebayo, A. I. (2020). Repurposing of chloroquine and some clinically approved antiviral drugs as effective therapeutics to prevent cellular entry and replication of coronavirus. *Journal of Biomolecular Structure and Dynamics (Just-Accepted)*, 1–14. https://doi.org/10.1080/07391102.2020.1765876

Al-Khafaji, K., Al-DuhaidahawiL, D., & Taskin Tok, T. (2020). Using integrated computational approaches to identify safe and rapid treatment for SARS-CoV-2. *Journal of Biomolecular Structure and Dynamics (Just-Accepted)*, 1–11. https://doi.org/10.1080/07391102.2020.1764392

Aydin, H., Al-Khooly, D., & Lee, J. E. (2014). Influence of hydrophobic and electrostatic residues on SARS-coronavirus S2 protein stability: insights into mechanisms of general viral fusion and inhibitor design. *Protein Science: A Publication of the Protein Society*, 23(5), 603–617. https://doi.org/10.1002/pro.2442

Boopathi, S., Poma, A. B., & Kolandaivel, P. (2020). Novel 2019 Coronavirus structure, mechanism of action, antiviral drug promises and rule out against its treatment. *Journal of Biomolecular Structure and Dynamics (Just-Accepted)*, 1–14. https://doi.org/10.1080/07391102.2020.1758788

Elfiky, A. A. (2020a). Natural products may interfere with SARS-CoV-2 attachment to the host cell. *Journal of Biomolecular Structure and Dynamics (Just-Accepted)*, 1–16. https://doi.org/10.1080/07391102.2020.1761881

Elfiky, A. A. (2020b). SARS-CoV-2 RNA dependent RNA polymerase (RdRp) targeting: An in silico perspective. *Journal of Biomolecular Structure and Dynamics (Just-Accepted)*, 1–15. https://doi.org/10.1080/07391102.2020.1761882

Elmezayen, A. D., Al-Obaidi, A., Şahin, A. T., & Yelekçi, K. (2020). Drug repurposing for coronavirus (COVID-19): In silico screening of known drugs against coronavirus 3CL hydrolase and protease enzymes. *Journal of Biomolecular Structure and Dynamics (Just-Accepted)*, 1–12. https://doi.org/10.1080/07391102.2020.1758791

Enayatkhani, M., Hasaniazad, M., Faezi, S., Guklani, H., Davoodian, P., Ahmadi, N., Einakian, M. A., Karmostaji, A., & Ahmadi, K. (2020). Reverse vaccinology approach to design a novel multi-epitope vaccine candidate against COVID-19: An in silico study. *Journal of Biomolecular Structure and Dynamics (Just-Accepted)*, 1–19. https://doi.org/10.1080/07391102.2020.1756411

Guo, Z., Mohanty, U., Noehre, J., Sawyer, T. K., Sherman, W., & Krilov, G. (2010). Probing the alpha-helical structural stability of stapled p53 peptides: molecular dynamics simulations and analysis. *Chemical Biology & Drug Design*, 75(4), 348–359. https://doi.org/10.1111/j.1747-0285.2010.00951.x

Gupta, M. K., Vemula, S., Donde, R., Gouda, G., Behera, L., & Vadde, R. (2020). In-silico approaches to detect inhibitors of the human severe acute respiratory syndrome coronavirus envelope protein ion channel.

Journal of Biomolecular Structure and Dynamics (Just-Accepted), 1–17. https://doi.org/10.1080/07391102.2020.1751300

Han, D. P., Penn-Nicholson, A., & Cho, M. W. (2006). Identification of critical determinants on ACE2 for SARS-CoV entry and development of a potent entry inhibitor. *Virology*, 350(1), 15–25. https://doi.org/10.1016/j.virol.2006.01.029

Hasan, A., Paray, B. A., Hussain, A., Qadir, F. A., Attar, F., Aziz, F. M., Sharifi, M., Derakhshankhah, H., Rasti, B., & Mehrabi, M. (2020). A review on the cleavage priming of the spike protein on coronavirus by angiotensin-converting enzyme-2 and furin. *Journal of Biomolecular Structure and Dynamics (Just-Accepted)*, 1–13. https://doi.org/10.1080/07391102.2020.1754293

Islam, R., Parves, R., Paul, A. S., Uddin, N., Rahman, M. S., Mamun, A. A., Hossain, M. N., Ali, M. A., & Halim, M. A. (2020). A molecular modeling approach to identify effective antiviral phytochemicals against the main protease of SARS-CoV-2. *Journal of Biomolecular Structure and Dynamics (Just-Accepted)*, 1–20. https://doi.org/10.1080/07391102.2020.1761883

Jeffrey, G. A., & Jeffrey, G. A. (1997). *An introduction to hydrogen bonding* (Vol. 12). Oxford University Press. https://books.google.com.au/books?id=Gy29QgAACAAJ

Jorgensen, W. L., Maxwell, D. S., & Tirado-Rives, J. (1996). Development and testing of the OPLS all-atom force field on conformational energetics and properties of organic liquids. *Journal of the American Chemical Society*, 118(45), 11225–11236. https://doi.org/10.1021/ja9621760

Joshi, R. S., Jagdale, S. S., Bansode, S. B., Shankar, S. S., Tellis, M. B., Pandya, V. K., Chugh, A., Giri, A. P., & Kulkarni, M. J. (2020). Discovery of potential multi-target-directed ligands by targeting host-specific SARS-CoV-2 structurally conserved main protease$. *Journal of Biomolecular Structure and Dynamics (Just-Accepted)*, 1–16. https://doi.org/10.1080/07391102.2020.1760137

Khan, R. J., Jha, R. K., Amera, G., Jain, M., Singh, E., Pathak, A., Singh, R. P., Muthukumaran, J., & Singh, A. K. (2020). Targeting SARS-Cov-2: A systematic drug repurposing approach to identify promising inhibitors against 3C-like Proteinase and 2′-O-RiboseMethyltransferase. *Journal of Biomolecular Structure and Dynamics (Just-Accepted)*, 1–40. https://doi.org/10.1080/07391102.2020.1753577

Khan, S. A., Zia, K., Ashraf, S., Uddin, R., & Ul-Haq, Z. (2020). Identification of chymotrypsin-like protease inhibitors of SARS-CoV-2 via integrated computational approach. *Journal of Biomolecular Structure and Dynamics (Just-Accepted)*, 1–13. https://doi.org/10.1080/07391102.2020.1751298

Kumar, D., Kumari, K., Jayaraj, A., Kumar, V., Kumar, R. V., Dass, S. K., Chandra, R., & Singh, P. (2020). Understanding the binding affinity of noscapines with protease of SARS-CoV-2 for COVID-19 using MD simulations at different temperatures. *Journal of Biomolecular Structure and Dynamics*, 1–14. https://doi.org/10.1080/07391102.2020.1752310

Lan, J., Ge, J., Yu, J., Shan, S., Zhou, H., Fan, S., Zhang, Q., Shi, X., Wang, Q., Zhang, L., & Wang, X. (2020). Structure of the SARS-CoV-2 spike receptor-binding domain bound to the ACE2 receptor. *Nature*, 581(7807), 215–219. https://doi.org/10.1038/s41586-020-2180-5

Lobo-Galo, N., Terrazas-López, M., Martínez-Martínez, A., & Díaz-Sánchez, Á. G. (2020). FDA-approved thiol-reacting drugs that potentially bind into the SARS-CoV-2 main protease, essential for viral replication. *Journal of Biomolecular Structure and Dynamics (Just-Accepted)*, 1–12. https://doi.org/10.1080/07391102.2020.1764393

Lu, R., Zhao, X., Li, J., Niu, P., Yang, B., Wu, H., Wang, W., Song, H., Huang, B., Zhu, N., Bi, Y., Ma, X., Zhan, F., Wang, L., Hu, T., Zhou, H., Hu, Z., Zhou, W., Zhao, L., … Tan, W. (2020). Genomic characterisation and epidemiology of 2019 novel coronavirus: Implications for virus origins and receptor binding. *The Lancet*, 395(10224), 565–574. https://doi.org/10.1016/S0140-6736(20)30251-8

Muralidharan, N., Sakthivel, R., Velmurugan, D., & Gromiha, M. M. (2020). Computational studies of drug repurposing and synergism of lopinavir, oseltamivir and ritonavir binding with SARS-CoV-2 protease against COVID-19. *Journal of Biomolecular Structure and Dynamics (Just-Accepted)*, 1–7. https://doi.org/10.1080/07391102.2020.1752802

Pant, S., Singh, M., Ravichandiran, V., Murty, U., & Srivastava, H. K. (2020). Peptide-like and small-molecule inhibitors against Covid-19. *Journal of Biomolecular Structure and Dynamics (Just-Accepted)*, 1–15. https://doi.org/10.1080/07391102.2020.1757510

Peeri, N. C., Shrestha, N., Rahman, M. S., Zaki, R., Tan, Z., Bibi, S., Baghbanzadeh, M., Aghamohammadi, N., Zhang, W., & Haque, U. (2020). The SARS, MERS and novel coronavirus (COVID-19) epidemics, the newest and biggest global health threats: What lessons have we learned? *International Journal of Epidemiology*, 1–10. https://doi.org/10.1093/ije/dyaa033

Sarma, P., Sekhar, N., Prajapat, M., Avti, P., Kaur, H., Kumar, S., Singh, S., Kumar, H., Prakash, A., & Dhibar, D. P. (2020). In-silico homology assisted identification of inhibitor of RNA binding against 2019-nCoV N-protein (N terminal domain). *Journal of Biomolecular Structure and Dynamics (Just-Accepted)*, 1–11. https://doi.org/10.1080/07391102.2020.1753580

Sastry, G. M., Adzhigirey, M., Day, T., Annabhimoju, R., & Sherman, W. (2013). Protein and ligand preparation: Parameters, protocols, and influence on virtual screening enrichments. *Journal of Computer-Aided Molecular Design*, 27(3), 221–234. https://doi.org/10.1007/s10822-013-9644-8

Sinha, S. K., Shakya, A., Prasad, S. K., Singh, S., Gurav, N. S., Prasad, R. S., & Gurav, S. S. (2020). An in-silico evaluation of different Saikosaponins for their potency against SARS-CoV-2 using NSP15 and fusion spike glycoprotein as targets. *Journal of Biomolecular Structure and Dynamics (Just-Accepted)*, 1–13. https://doi.org/10.1080/07391102.2020.1762741

Tina, K., Bhadra, R., & Srinivasan, N. (2007). PIC: Protein interactions calculator. *Nucleic Acids Research*, 35(Web Server issue), W473–W476. https://doi.org/10.1093/nar/gkm423

Umesh, K., D., Selvaraj, C., Singh, S. K., & Dubey, V. K. (2020). Identification of new anti-nCoV drug chemical compounds from Indian spices exploiting SARS-CoV-2 main protease as target. *Journal of Biomolecular Structure and Dynamics (Just-Accepted)*, 1–9. https://doi.org/10.1080/07391102.2020.1763202

Veeramachaneni, G. K., Raj, K. K., Chalasani, L. M., Annamraju, S. K., Js, B., & Talluri, V. R. (2015). Shape based virtual screening and molecular docking towards designing novel pancreatic lipase inhibitors. *Bioinformation*, 11(12), 535–542. https://doi.org/10.6026/97320630011535

Veeramachaneni, G. K., Raj, K. K., Chalasani, L. M., Bondili, J. S., & Talluri, V. R. (2015). High-throughput virtual screening with e-pharmacophore and molecular simulations study in the designing of pancreatic lipase inhibitors. *Drug Design, Development and Therapy*, 9, 4397–4412. https://doi.org/10.2147/DDDT.S84052

Veeramachaneni, G. K., Thunuguntla, V. B. S. C., Bhaswant, M., Mathai, M. L., & Bondili, J. S. (2019). Pharmacophore directed screening of agonistic natural molecules showing affinity to 5HT2C receptor. *Biomolecules*, 9(10), 556. https://doi.org/10.3390/biom9100556

Wahedi, H. M., Ahmad, S., & Abbasi, S. W. (2020). Stilbene-based natural compounds as promising drug candidates against COVID-19. *Journal of Biomolecular Structure and Dynamics (Just-Accepted)*, 1–16. https://doi.org/10.1080/07391102.2020.1762743

Wan, Y., Shang, J., Graham, R., Baric, R. S., & Li, F. (2020). Receptor recognition by the novel coronavirus from Wuhan: An analysis based on decade-long structural studies of SARS coronavirus. *Journal of Virology*, 94(7), 1–9. https://doi.org/10.1128/JVI.00127-20

WHO. (2020). *Coronavirus disease (COVID-2019) situation reports*. Retrieved April 23, 2020, from https://www.who.int/emergencies/diseases/novel-coronavirus-2019/situation-reports/

Yan, R., Zhang, Y., Li, Y., Xia, L., Guo, Y., & Zhou, Q. (2020). Structural basis for the recognition of SARS-CoV-2 by full-length human ACE2. *Science (New York, N.Y.)*, 367(6485), 1444–1448. https://doi.org/10.1126/science.abb2762

Zhou, G., & Zhao, Q. (2020). Perspectives on therapeutic neutralizing antibodies against the Novel Coronavirus SARS-CoV-2. *International Journal of Biological Sciences*, 16(10), 1718–1723. https://doi.org/10.7150/ijbs.45123